Stochastic Environmental Research and Risk Assessment 15 (2001) 65–86 © Springer-Verlag 2001

Error covariance modeling in sequential data assimilation

J. Sénégas, H. Wackernagel, W. Rosenthal, T. Wolf

Abstract. The efficiency of a sequential data assimilation scheme relies on the capability to describe the error covariance. This aspect is all the more relevant if one needs accurate statistics on the estimation error. Frequently an ad hoc function depending on a few parameters is proposed, and these parameters are tuned, estimated or updated. This usually requires that the covariance is second-order stationary (i.e. depends only on the distance between two points). In this paper, we discuss this feature and show that even in simple applications (such as one-dimensional hydrodynamics), this assumption does not hold and may lead to poorly described estimation errors. We propose a method relying on the analysis of the error term and the use of the hydrodynamical model to generate one part of the covariance function, the other part being modeled using a second-order stationary approach. This method is discussed using a twin experiment in the case where a physical parameter is erroneous, and improves significantly the results: the model bias is strongly reduced and the estimation error is well described. Moreover, it enables a better adaptation of the Kalman gain to the actual estimation error.

1 Introduction

Since computation for large numerical systems is not a challenge anymore, sequential data assimilation, which consists in correcting a model estimate with measurements according to a statistical criterion, i.e. the minimization of the estimation error variance, has been widely used in meteorology and hydrodynamics. Much effort has been invested in the last few years in setting up efficient algorithms to solve the estimation problem. Robustness, convergence to a steady state, extension to non-linear systems, etc. have been largely described (Maybeck,

J. Sénégas (✉), H. Wackernagel
Centre de Géostatistique, Ecole des Mines de Paris,
F-77305 Fontainebleau, France
Fax: +33-1-64-69-47-05,
e-mail: senegas@cg.ensmp.fr

W. Rosenthal, T. Wolf
Institute for Hydrophysics, GKSS Research Centre,
D-21502 Geesthacht, Germany

This work has been supported by the EC funded MAST III project PIONEER.

1979; Todling and Cohn, 1994; Evensen, 1995; Eigbe et al., 1998, Verlaan, 1998) and have led to many applications.

Recently, it appears that the extension to more sophisticated models, such as three dimensional hydrodynamical models (Cañizares, 1999), highly non-linear dynamical systems (Evensen and van Leeuwen, 1999; Verlaan and Heemink, 1999) or ecological models (Eknes and Evensen, 1999), has been of major interest and extensive work is still going on to implement numerical schemes capable of coping with the challenging non-linearity of applications in these fields. A few studies set focus on the statistical aspects of sequential data assimilation. Dee and da Silva (1998) question the assumption of non-bias of the first guess, arguing that a bias in the model ends in biased analyzed estimates, and propose a scheme to remove explicitly the bias. Other algorithms have been used to update the error covariance function by estimating on-line parameters such as correlation length or variance and to provide better statistics for the assimilation (Dee, 1992, 1995).

The reflection on the modeling of the error statistics is motivated by the following problem: to be operational, the Kalman filter requires principally the knowledge of the two first moments (mean and covariance) of the system error. However, it turns out very difficult in practice to have an idea of these statistical properties, since the true state is never known and perfect statistics cannot be computed. This problem gets more acute when there are few measurements in geographical space as this is the case in several hydrodynamical monitoring systems. In many applications, an ad hoc function, based often on exponential or powerlaw functions depending only on the distance, is proposed to model the error covariance, and a certain number of parameters are estimated or tuned to offer the best results (Evensen, 1992; Dee, 1995; Verlaan, 1998; Dee and da Silva, 1999; Dee et al. 1999). But the choice of the function itself and especially the validity of the second-order stationarity assumption are let somehow aside. This may be due to the fact that when data is plenty (like water level in hydrodynamical systems), the form of the covariance function may not influence very much the assimilation. Nevertheless, we think that a data assimilation system requires an extensive comprehension and a correct statistical description of the physical error terms.

In this paper, we focus on the modeling of the error covariance, and show that the assumptions implicitly made on the behavior of the random variables, such as second-order stationarity, are likely not to hold in many applications. For this purpose, we refer to the theory of regionalized variables used in geostatistics which has been successfully applied in earth sciences (Chilès and Delfiner, 1999). In the data assimilation literature, a covariance depending only on the distance between two points is usually said to be *homogeneous* (e.g. Gaspari and Cohn, 1999); we prefer the equivalent geostatistical qualificative *second-order stationary*, whatsoever the number of dimensions, whereas Yaglom (1986) reserves the latter for covariance functions in one dimension. In Sect. 2, we show that the estimation problem solved in sequential data assimilation is similar to a cokriging of the innovations, which enables us to apply the geostatistical tools to the problems encountered in data assimilation. We also present in this section a method to model the covariance error, which is based on a separation of the system noise into a physically interpretable term and a small-scale error. This method is discussed using a twin experiment with a linear one-dimensional hydrodynamical model and a reference state simulated by a shallow water flow model. The error in the linear model stems principally from an erroneous friction coefficient. The choice of a linear model is motivated by the fact that in this case the Kalman filter is supposed to work well, but the approach presented here can be extended to

non-linear systems. Section 3 introduces the equations of the shallow water model used as reference and its linearized counterpart. Results of data assimilation are given in Sect. 4. We show that the assumption of second-order stationarity does not hold and leads to strongly biased estimates and to a poor prediction of the estimation error. The dynamical modeling introduced in Sect. 2 improves consequently the estimates and provides an accurate description of the estimation error.

2
A geostatistical approach of data assimilation

In this section, we emphasize the equivalence between kriging and Kalman filtering. While Kalman filtering has gained increasing popularity in atmospheric and hydrodynamical modeling (Daley, 1991; Bennett, 1992), geostatistics has spread in the earth sciences (Journel and Huijbregts, 1978; Chilès and Delfiner, 1999), where a variable has to be estimated from spatially distributed samples at a fixed time. Geostatistics offers a general frame to study regionalized variables (i.e. arbitrary functions of a multidimensional space) considered as realizations of random functions. Those two approaches, Kalman filtering and kriging (the first one stemming from control theory, whereas the second one from the theory of regionalized variables) provide equivalent solutions to the estimation problem encountered in data assimilation. In this section, we show that the analysis step in Kalman filtering can be regarded as the cokriging of the first guess error.

2.1
The analysis scheme

We consider the estimation problem posed in data assimilation and will use a cokriging method to establish the equations of the so-called *analysis scheme*.

We want to estimate the true state $\mathbf{z}$ of a system from an observation $\mathbf{z}^o$ and on the basis of a first guess $\mathbf{z}^f$ of the true state. In this approach, $\mathbf{z}$, $\mathbf{z}^o$ and $\mathbf{z}^f$ are random vectors, whose components are the physical variables of the system at different locations. This is therefore a multivariate and multisite framework.

The true state $\mathbf{z}$ will be estimated on a grid with n nodes and the corresponding first guess vector $\mathbf{z}^f$ is of the same size. There are m observations available in a vector $\mathbf{z}^o$. In practice, m is much smaller than n, and we shall assume that the observation locations are a subset of the grid nodes. The relation between estimation nodes and observation nodes is described by the observation matrix $\mathbf{L}$: a multiplication by the matrix $\mathbf{L}$ of size $m \times n$ projects an n-vector to a corresponding m-vector. In the sequel, $\mathbf{x}$ will refer to a grid node, while α will be used to denote observation points.

We now introduce the first guess error $\mathbf{y}^f$ and the observational error $\mathbf{y}^o$ as additive noise:

$$\mathbf{z}^f = \mathbf{z} + \mathbf{y}^f \tag{1}$$

$$\mathbf{z}^o = \mathbf{L}\mathbf{z} + \mathbf{y}^o \tag{2}$$

We assume that these stochastic error terms are known with their first and second moments. Replacing without loss of generality the random variables by their centered counterparts if necessary (this is possible since the first moment is known), we can write

$$\overline{\mathbf{y}^f} = 0 \quad \overline{\mathbf{y}^o} = 0 \tag{3}$$

$$\overline{\mathbf{y}^{\mathrm{f}}(\mathbf{y}^{\mathrm{f}})^{\mathrm{T}}} = \mathbf{C}^{\mathrm{f}} \quad \overline{\mathbf{y}^{\mathrm{o}}(\mathbf{y}^{\mathrm{o}})^{\mathrm{T}}} = \mathbf{C}^{\mathrm{o}} \tag{4}$$

where the overbar is the expectation operator, $\mathbf{C}^{\mathrm{f}}$ and $\mathbf{C}^{\mathrm{o}}$ are the $n \times n$ and $m \times m$ variance–covariance matrices of the first guess and the observational errors.

We assume moreover that the first guess and the observational noises are uncorrelated, i.e.

$$\overline{\mathbf{y}^{\mathrm{o}}(\mathbf{L}\mathbf{y}^{\mathrm{f}})^{\mathrm{T}}} = 0 \tag{5}$$

Equations (1)–(5) constitute the estimation problem as introduced in the analysis step of data assimilation (see Evensen, 1992 for a more detailed introduction). Note that Eq. (3) is often referred to as the non-bias assumption.

The regionalized variable we consider is the first guess error $\mathbf{y}^{\mathrm{f}}$. Since we do not observe directly the realizations of $\mathbf{y}^{\mathrm{f}}$, the first guess error will be estimated from $\mathbf{z}^{\mathrm{o}}$ and $\mathbf{L}\mathbf{z}^{\mathrm{f}}$. Therefore, the unbiased linear estimate $\mathbf{y}^{*}$ takes the following form:

$$\mathbf{y}^{*} = \mathbf{\Lambda}(\mathbf{L}\mathbf{z}^{\mathrm{f}} - \mathbf{z}^{\mathrm{o}}) \tag{6}$$

where $\mathbf{\Lambda}$ is the matrix of the weights. The difference $\mathbf{z}^{\mathrm{o}} - \mathbf{L}\mathbf{z}^{\mathrm{f}}$ is usually called the innovation.

We now denote y_x^* the optimal estimate of $\mathbf{y}^{\mathrm{f}}$ at position $\mathbf{x}$. Since we consider a random function for which the first and second moments are defined, we can use a simple cokriging method (see Wackernagel, 1998 for more details). The estimation problem is then solved by minimizing without constraint the variance of the estimation error:

$$\mathrm{Var}\left(y_x^* - y_x^{\mathrm{f}}\right) = \sum_{\alpha\beta} \lambda_{\alpha x} C_{\alpha\beta} \lambda_{\beta x} - 2 \sum_{\alpha} \lambda_{\alpha x} C_{\alpha x} + C_{xx} \tag{7}$$

The covariances in this expression can be written as

$$C_{\alpha\beta} = \mathrm{Cov}\left(y_\alpha^{\mathrm{f}} - y_\alpha^{\mathrm{o}}, y_\beta^{\mathrm{f}} - y_\beta^{\mathrm{o}}\right) = \left(\mathbf{L}\mathbf{C}^{\mathrm{f}}\mathbf{L}^{\mathrm{T}} + \mathbf{C}^{\mathrm{o}}\right)_{\alpha\beta} \tag{8}$$

$$C_{\alpha x} = \mathrm{Cov}\left(y_\alpha^{\mathrm{f}} - y_\alpha^{\mathrm{o}}, y_x^{\mathrm{f}}\right) = \left(\mathbf{L}\mathbf{C}^{\mathrm{f}}\right)_{\alpha x} \tag{9}$$

$$C_{xx} = \mathrm{Var}\left(y_x^{\mathrm{f}}\right) = \left(\mathbf{C}^{\mathrm{f}}\right)_{xx} \tag{10}$$

The minimization of expression (7) for every grid node $\mathbf{x}$ leads to the resolution of a linear system, which can be written in matrix form

$$\left(\mathbf{C}_{\alpha\beta}\right)\left(\mathbf{\Lambda}_{\beta x}\right) = \left(\mathbf{C}_{\alpha x}\right) \tag{11}$$

where the subscripts indicate the domain of definition of the matrix.

The solution can then be computed from this equation by inversion of the matrix $\left(\mathbf{C}_{\alpha\beta}\right)$. This matrix being a covariance matrix, it is positive semi-definite. The vector of estimates $\mathbf{y}^{*}$ for the whole domain can then be written as

$$\mathbf{y}^{*} = \left(\mathbf{C}_{\alpha x}\right)^{\mathrm{T}}\left(\mathbf{C}_{\alpha\beta}\right)^{-1}\left(\mathbf{L}\mathbf{z}^{\mathrm{f}} - \mathbf{z}^{\mathrm{o}}\right) \tag{12}$$

The variance–covariance matrix associated with this estimate is then obtained by replacing the solution of Eq. (11) into Eq. (7):

$$\mathrm{Cov}\left(\mathbf{y}^* - \mathbf{y}^{\mathrm{f}}\right) = \mathbf{C}_{xx} - \mathbf{C}_{\alpha x}^{\mathrm{T}}\mathbf{C}_{\alpha\beta}^{-1}\mathbf{C}_{\alpha x} \tag{13}$$

Therefore, using Eqs. (1) and (2) and the relations established in (8)–(10), the analyzed estimate $\mathbf{z}^*$ of the state $\mathbf{z}$ takes the form

$$\mathbf{z}^* = \mathbf{z}^{\mathrm{f}} - \mathbf{y}^* = \mathbf{z}^{\mathrm{f}} + \mathbf{C}^{\mathrm{f}}\mathbf{L}^{\mathrm{T}}\left(\mathbf{L}\mathbf{C}^{\mathrm{f}}\mathbf{L}^{\mathrm{T}} + \mathbf{C}^{\mathrm{o}}\right)^{-1}\left(\mathbf{z}^{\mathrm{o}} - \mathbf{L}\mathbf{z}^{\mathrm{f}}\right) \tag{14}$$

and the variance–covariance matrix of the estimation error is given by

$$\mathrm{Cov}(\mathbf{z}^* - \mathbf{z}) = \mathbf{C}^{\mathrm{f}} - \mathbf{C}^{\mathrm{f}}\mathbf{L}^{\mathrm{T}}\left(\mathbf{L}\mathbf{C}^{\mathrm{f}}\mathbf{L}^{\mathrm{T}} + \mathbf{C}^{\mathrm{o}}\right)^{-1}\mathbf{L}\mathbf{C}^{\mathrm{f}} \tag{15}$$

These two equations represent the analysis scheme in the Kalman filter: this step is therefore equivalent in geostatistical terms to the cokriging of the first guess error.

In this approach, we hid somehow the multivariate nature of the problem through the use of a state variable $\mathbf{z}$. This has been possible through the assumption of non-bias; indeed, with Eq. (3), the condition of universality (or of non-bias of the estimates) is automatically fulfilled and there is no need to distinguish between the variables and the sites in the notation.

Finally, we write down the Kalman filter equations used in sequential data assimilation

$$\mathbf{z}_k^{\mathrm{f}} = f_k\left(\mathbf{z}_{k-1}^*, \mathbf{u}_k\right) \tag{16}$$

$$\mathbf{C}_k^{\mathrm{f}} = \mathbf{F}_k\mathbf{C}_{k-1}^*\mathbf{F}_k^{\mathrm{T}} + \mathbf{Q}_k \tag{17}$$

$$\mathbf{K}_k = \mathbf{C}_k^{\mathrm{f}}\mathbf{L}^{\mathrm{T}}\left(\mathbf{L}\mathbf{C}_k^{\mathrm{f}}\mathbf{L}^{\mathrm{T}} + \mathbf{C}^{\mathrm{o}}\right)^{-1} \tag{18}$$

$$\mathbf{z}_k^* = \mathbf{z}_k^{\mathrm{f}} + \mathbf{K}_k\left(\mathbf{z}_k^{\mathrm{o}} - \mathbf{L}\mathbf{z}_k^{\mathrm{f}}\right) \tag{19}$$

$$\mathbf{C}_k^* = (\mathbf{I}_n - \mathbf{K}_k\mathbf{L})\mathbf{C}_k^{\mathrm{f}} \tag{20}$$

where $\mathbf{F}_k$ is the linearization of the model operator f_k, $\mathbf{u}_k$ a forcing term, $\mathbf{Q}_k$ the covariance matrix of the *system noise* $\mathbf{q}_k$, $\mathbf{I}_n$ the identity matrix of $\mathbb{R}^n$ and the subscript k indicates that the variable is considered at time k.

2.2 Covariance modeling

The issue raised by the estimation of the system noise is actually a central point in the implementation of data assimilation. The propagation equation (17) states that only the system noise has to be modeled, the first guess error being computed by the algorithm. In that sense, the Kalman filter can be regarded as a powerful tool to generate a covariance structure, when this one is highly dependent on the dynamical process. In practice, however, the system noise introduced in Eq. (17) cannot be computed directly from the innovations, and must be evaluated with other techniques.

In many applications, it is reasonable to reduce the system error to a noise in specific variables and to model the influence of this uncertainty on the state variables. Denoting $\mathbf{G}_k$ such an operator, we have the following relation:

$$\mathbf{q}_k = \mathbf{G}_k \tilde{\mathbf{q}}_k \tag{21}$$

where $\tilde{\mathbf{q}}_k$ is the reduced noise vector. Cañizares (1999) reviews the different sources of uncertainty in hydrodynamical applications and proposes to consider the errors in the forcing terms (wind field, boundary conditions, etc.), in the model parameters (e.g. friction coefficients) and in the model description (coarse discretization, poorly described physics, etc.). The resulting system noise covariance matrix is given by

$$\mathbf{Q}_k = \mathbf{G}_k \tilde{\mathbf{Q}}_k \mathbf{G}_k^{\mathrm{T}} \tag{22}$$

where $\tilde{\mathbf{Q}}_k = \overline{\tilde{\mathbf{q}}_k \tilde{\mathbf{q}}_k^{\mathrm{T}}}$.

Frequently a spatial structure is proposed for the covariance $\tilde{\mathbf{Q}}_k$ from the knowledge of the physics and this model is validated a posteriori. This step requires a prior fitting of the stochastic parameters, such as correlation length or standard deviation. This method is known as covariance matching and consists mainly in comparing at the locations, where data are available the estimation error covariance estimated by the filter with the true covariance (see Dee, 1995; Verlaan, 1998). This in turn can only be done if the number of parameters is small enough to be tractable and justifies the use of second-order stationary covariances. Note that this is not only a practical limitation, but also a theoretical one; for the sake of parsimony it makes no sense to propose a covariance structure whose complexity cannot be justified.

The relevance of a second-order stationary covariance model is an important issue. We think that it is an assumption which should first be checked on the available data. In Sect. 4, the case where the model estimate is perturbed by an error in a physical parameter will be studied and we will show that the resulting system error covariance cannot be considered second-order stationary. It is possible to cope with this difficulty by increasing the system error variance, but this solution is not really appropriate.

Using the dynamical model to compute the system noise covariance proves then to be a powerful alternative. Let α be a parameter of the model, so that we can write

$$\mathbf{z}_{k+1} = f(\mathbf{z}_k, \alpha) \tag{23}$$

Denoting q_α an error in the parameter, we have the following relation:

$$f(\mathbf{z}_k, \alpha + q_\alpha) \approx f(\mathbf{z}_k, \alpha) + q_\alpha \frac{\partial f}{\partial q_\alpha}(\mathbf{z}_k, \alpha) \tag{24}$$

Therefore, the resulting model error can be computed using an approximation of the derivative of f with respect to q_α around the state $\mathbf{z}_k$

$$\mathbf{q}_k = \frac{1}{\varepsilon}(f(\mathbf{z}_k, \alpha + \varepsilon q_\alpha) - f(\mathbf{z}_k, \alpha)) \tag{25}$$

with ε a real verifying $|\varepsilon| \ll 1$.

The linear operator $\mathbf{G}_k$ introduced in Eq. (21) can then be easily computed from the numerical model f

$$\mathbf{G}_k s = \frac{1}{\varepsilon}\left(f(\mathbf{z}_k, \alpha + \varepsilon s) - f(\mathbf{z}_k, \alpha)\right) \tag{26}$$

We propose here to combine both approaches. For this purpose, we consider the system noise to be the sum of two independent random variables

$$\mathbf{q}_k = \mathbf{G}_k \tilde{\mathbf{q}}_k + \mathbf{q}_k^{\text{stat}} \tag{27}$$

where $\tilde{\mathbf{q}}$ accounts for the noise in physical parameters and $\mathbf{q}_k^{\text{stat}}$ is the second-order stationary part of the system noise $\mathbf{q}_k$. In this approach, $\mathbf{q}_k^{\text{stat}}$ accounts for the noise which cannot be directly linked to an error in the physics. Although the hypothesis of second-order stationarity is above all a practical simplification, which turns out almost necessary if one wants to model the spatial structure, the approach proposed here seems reasonable if one considers that the large scale part of the system error, whose spatial structure is complex, is due to uncertainties in the physics. The low-scale behavior is then likely to be described with a second-order stationary model. Note nevertheless that such a dichotomy is arbitrary, and especially, is not unique.

Both random variables being independent, the total system error covariance is given by the relation

$$\mathbf{Q}_k = \mathbf{G}_k \tilde{\mathbf{Q}}_k \mathbf{G}_k^{\mathrm{T}} + \mathbf{Q}_k^{\text{stat}} \tag{28}$$

Typically, the modeling of the second-order stationary covariance $\mathbf{Q}_k^{\text{stat}}$ implies beside the choice of a covariance model the estimation of a sill and a range. These two parameters can thus be evaluated by covariance matching. In Dee (1995), a scheme to update these parameters is proposed, based on the maximum likelihood estimator. Although such an algorithm may also be applied here, one may consider that the temporal variability is fully described by the covariance $\mathbf{G}_k \tilde{\mathbf{Q}}_k \mathbf{G}_k^{\mathrm{T}}$ in Eq. (28), since it is state dependent.

Especially, we would like to consider problems where only a few observations of the system are available. This is for example the case in hydrodynamical applications for shallow water flow where the area under study is relatively small: typically, the number of assimilated data is of the order of 10. In those cases, it is not advisable to use schemes accounting for model bias (Dee and da Silva, 1998) or updating covariance parameters, for which the number of available observations should exceed "the number of tunable parameters by two or three orders of magnitude" (Dee, 1995).

We propose now to illustrate the technique described above, which will be referred to as *dynamical covariance modeling*, using a twin experiment, in which a shallow water model describes flow in a one-dimensional channel.

3
The hydrodynamical model

We propose to illustrate the modeling techniques with a simple linear one-dimensional hydrodynamical model (Lin1D) describing shallow water flow in a channel. The true state will be simulated with a non-linear isotropic shallow water model, referred to as Trim1D.

The one-dimensional shallow water model Trim1D used as reference is based on the de Saint Venant equations and has been proposed by Casulli (1995). These equations will be later simplified to obtain a linear expression for the driving equations of Lin1D. In both versions of the hydrodynamic model, we will assume that the pressure is hydrostatic and will consider a channel with uniform depth H.

The shallow water model describes free surface flow of an incompressible fluid with constant density in the one-dimensional case. We denote u the fluid velocity averaged over the cross-section, η the laterally averaged free surface elevation, p the normalized pressure, i.e. the pressure divided by the constant density ρ, g the gravitational acceleration and ν an eddy viscosity coefficient. For commodity, we denote moreover ∂_s the differential operator with respect to the variable s, i.e. $\partial/\partial s$.

The de Saint Venant equations can be derived from the Navier–Stokes equations, which express the conservation of momentum and mass, by performing an average over the cross-section A:

$$\partial_t(Au) + \partial_x(Auu) = -gA\partial_x\eta + \partial_x(\nu A\partial_x u) - \gamma u \tag{29}$$

$$\partial_t A + \partial_x(Au) = 0 \tag{30}$$

with γ a friction coefficient taken to be

$$\gamma = H\frac{g\eta^2|u|}{R^{4/3}} \tag{31}$$

where R is the hydraulic radius (ratio of the cross-section area and the wet perimeter). With properly specified initial and boundary conditions, Eqs. (29) and (30) form a well-posed initial-boundary value problem for one-dimensional shallow water flow (Casulli and Cattani, 1992). Casulli (1995) proposes an algorithm for the discretization and the resolution of these equations, which has been used to compute the numerical solution of Trim1D in the case of a uniform depth H.

3.1 Linearization

A linear expression is now derived from the de Saint Venant equations. We neglect the viscosity terms in Eq. (29), i.e. we take $\nu = 0$. This assumption is fairly reasonable in open channel flows (Casulli, 1995). We choose to neglect the convection terms in Eq. (29) in comparison to the horizontal acceleration. We also neglect the horizontal gradient of the cross-section area in Eq. (30). This assumption is reasonable when the depth H is high compared to the water level elevations.

Bearing in mind that we consider a channel of uniform depth H, we obtain the following linear equations:

$$\partial_t u + g\partial_x\eta + c_f u = 0 \tag{32}$$

$$\partial_t\eta + H\partial_x u = 0 \tag{33}$$

where c_f is a steady friction coefficient. These equations form the one-dimensional linear model we will use as a first illustration of the data assimilation techniques.

3.2
Comparison of the two models for an open channel

Both models have been discretized on a regular grid using a semi-implicit method and we denote θ the implicitness parameter. We chose the following values for the model parameters:

H	L	c_f	Δt	Δx	T	θ
10 m	25 km	0.00085 s^{-1}	300 s	500 m	24 h	0.6

In all simulations we use the same boundary conditions describing an open channel: at one extremity, we impose for the water level elevation a periodic signal representing the sea boundary, and at the other one we will set the water level elevation to 0; the latter, e.g. occurs if the channel is connected to a large area of water, for which the water level can be considered steady. There is no boundary condition for the velocity. Therefore, we have for the two models

$$\eta_1(t) = 0.45 \sin\left(2\pi \frac{t}{12}\right) \tag{34}$$

$$\eta_{N_x}(t) = 0 \tag{35}$$

The initial conditions are

$$\eta(x, 0) = 0 \tag{36}$$

$$u(x, 0) = 0 \tag{37}$$

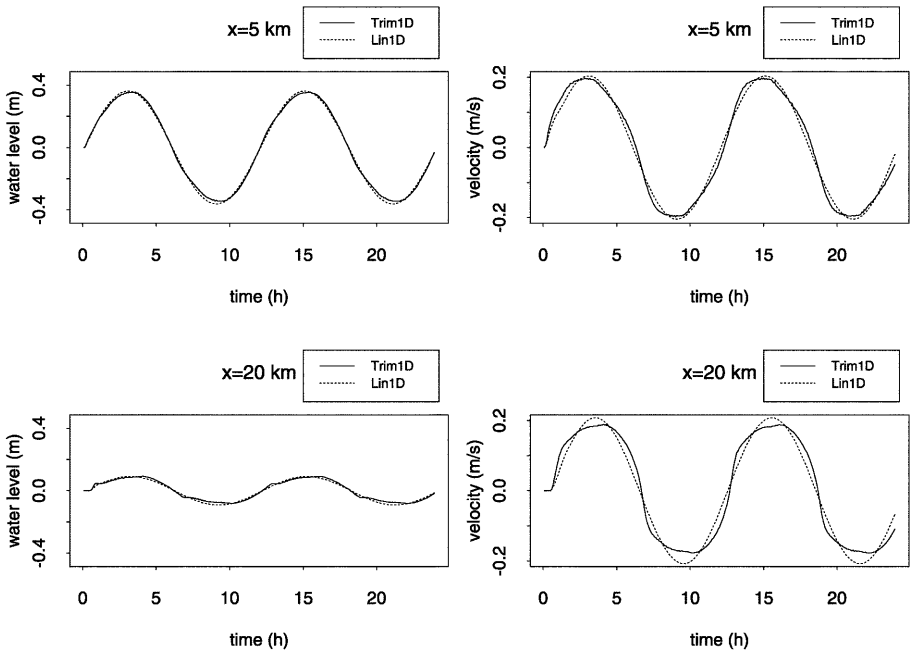

Fig. 1. Time series of water level (left) and velocity (right) for a one day run – comparison between Trim1D (solid line) and Lin1D (dashed line) for two different locations: $x = 5$ and 20 km

Figure 1 shows a one day time series of water level elevation and velocity for both models at two different locations ($x = 5$ and 20 km). At every location, you can observe the 12-h periodic sinus wave which enters the channel at $x = 0$. Note the decreasing amplitude of the water level elevation, which is due to the nature of the boundary conditions. In this application, the speed of the wave is approximately equal to 10 m s^{-1}, which means that within 42 min (about 9 model iterations), the signal has propagated through the channel. You may note this slight delay at the very beginning of the time series. The system is controlled by two forces principally: the water level gradient, which if positive implies an input of water in the system and on the other hand an output if negative, and the friction forces, which slow down the water flow. These two forces are approximately in balance.

Both models show very similar results. Especially, Lin1D neither underestimates nor overestimates systematically the true state. The slight differences which may be observed in comparing the velocities may be explained by the fact that a steady friction coefficient is used in Lin1D, while Trim1D calculates a state dependent coefficient, see Eq. (31).

3.3
Influence of an erroneous friction coefficient

In the previous case, the values of the physical parameters have been tuned so that both models provide similar results. It may be therefore interesting to consider the case where an error in the model parameters occurs and to use the data assimilation to correct this error.

In practice, physical parameters may be tuned by comparing the results of a model with measurements or may be even evaluated with a statistical method (see Evensen et al., 1998 for an overview). Nevertheless, if the number of parameters is relatively large, as can be the case in three-dimensional hydrodynamical models or in biological models, the data do not provide enough information to evaluate each parameter separately. Therefore, it may be preferable to model the global error due to uncertain parameters with a statistical approach and to use a filter to correct the model estimates.

For our application, we chose to simulate an error in the friction coefficient. As we want our example to be demonstrative, we used deliberately a very small value, i.e.

$$c_f = 0.0002\,s^{-1} \tag{38}$$

The results of the simulations performed with this new coefficient friction are shown in Fig. 2. The evolution of water level elevation is governed by the continuity equation (33), which has remained the same, and only depends on the spatial gradients of velocity. Since the gradients in this example are relatively small, the perturbation introduced by the erroneous coefficient is very small so that the results are quite similar to the previous run. The situation is different for velocity: the friction coefficient being now too low, the water level gradient forces are not balanced any more by the friction forces. Therefore, the velocity reaches higher values. Note especially that velocity and water level elevation are not in phase anymore, the velocity being maximal a little later than the water level elevation. This is in fact an important consequence, since now the linear model simulates water exchanges with the outside with a noticeable delay.

4
Correction through a data assimilation scheme

We propose to assimilate on the basis of the linear model Lin1D perturbed values from the reference shallow water model. Therefore, we simulate a measurement

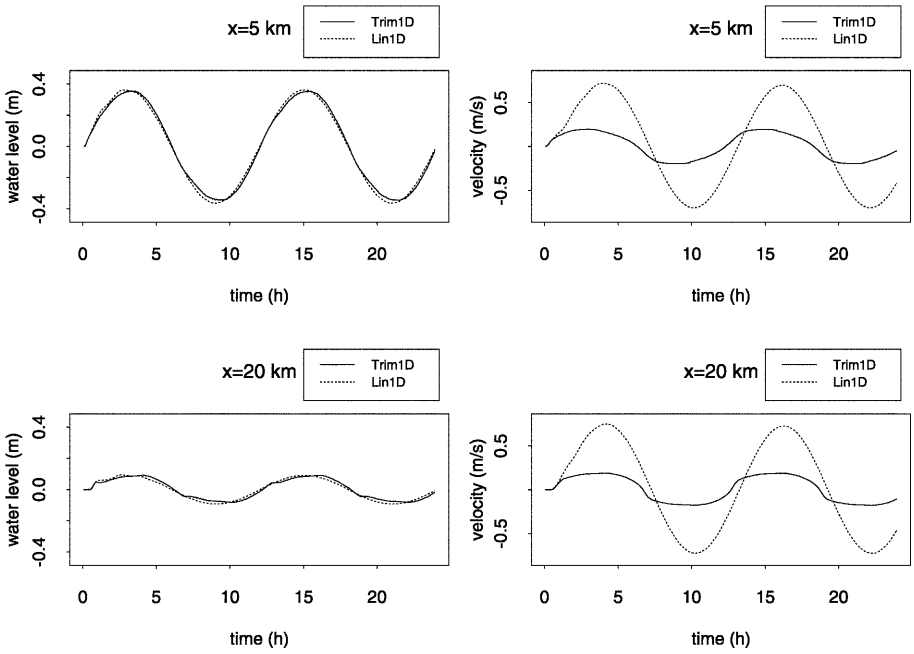

Fig. 2. Time series of water level (left) and velocity (right) for a one day run – comparison between Trim1D (solid line) and Lin1D (dashed line) for two different locations: $x = 5$ and 20 km. The friction coefficient is now too low, so that the friction forces do not balance the water level gradients any more, which ends in too large velocities

station located at the middle of the channel, so that one value for each variable (water level elevation, velocity) will be used. So as to simulate measurement error, we add a white noise (uncorrelated Gaussian noise) with a standard deviation of $\sigma_o = 0.005$ to both physical variables computed with Trim1D.

In real application studies, the measurement noise must be evaluated from the data. Note that the assumption of independent measurement errors is often made, so that only the variance is needed. Under the assumption of additive Gaussian noise, the variance can be easily computed from the time series of the measurement minus model forecast. Indeed, in that case, the noise variance appears as nugget-effect on the experimental variogram. Figure 3, which represents the behavior of the variogram at the origin, shows that using this method, a variance equal to 24×10^{-6} m has been computed for the measurements of water level elevation, which is very close to the real value 25×10^{-6} m used in the simulation.

In the sequel, the following measurement error covariance function will be used (the subscript w denotes a value related to water level, v to velocity):

$$C_w^o(h) = 25 \times 10^{-6} \delta(h) \tag{39}$$

$$C_v^o(h) = 25 \times 10^{-6} \delta(h) \tag{40}$$

where h represents the lag and $\delta(h)$ is a nugget-effect covariance function with a value of one for $|h| = 0$ and zero otherwise.

4.1
Second-order stationary system noise covariance

We now study in detail the spatial structure of the system noise. In Kalman filtering, the system noise $\mathbf{q}$ is introduced as an additive noise:

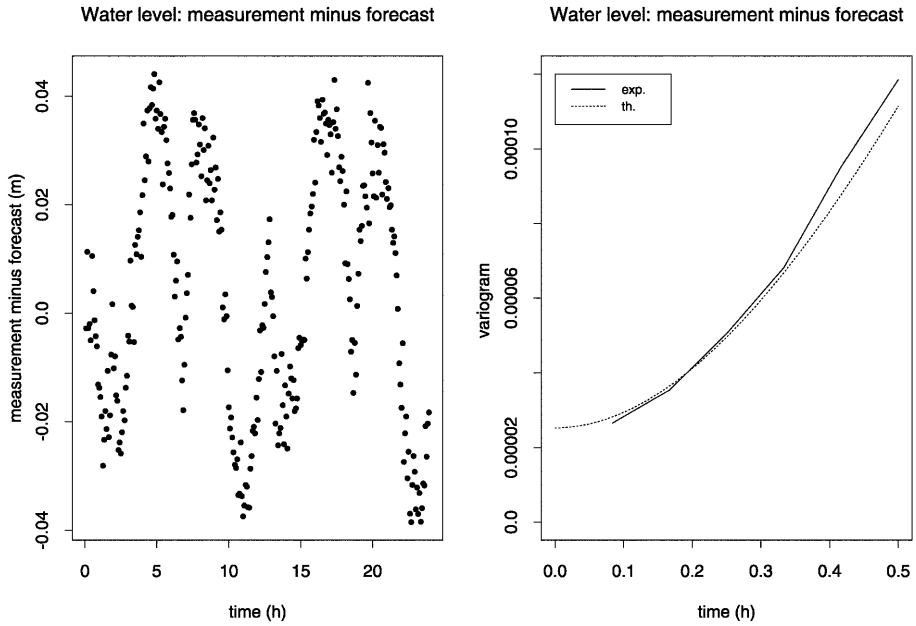

Fig. 3. The left plot shows the time series of simulated measurement minus model forecast for the water level elevation. On the right, the corresponding experimental (solid line) and theoretical (dashed line) variograms are plotted. The nugget-effect corresponds exactly to the variance of the measurement noise

$$\mathbf{z}_{k+1} = f(\mathbf{z}_k, \mathbf{u}_k) + \mathbf{q}_{k+1} \tag{41}$$

In our application, we are provided at any time with the full true state vector. It is thus possible to calculate at each step the real system error by computing the difference $\mathbf{z}_{k+1} - f(\mathbf{z}_k, \mathbf{u}_k)$, where f is Lin1D. Therefore, we will be able to study the structure of the system noise in the ideal case where it is known completely. Especially, we will question the stationarity hypothesis.

The modeling of the variogram structure is a practical problem for which an assumption of second-order stationarity may be suitable (yet this is not a necessity). This means in our case that the model error would be regarded as a second-order stationary random function. In order to check this hypothesis, experimental variograms are plotted and interpreted. The variograms are defined on the basis of the more general assumption of *intrinsic stationarity* (see, e.g. Wackernagel, 1998 or Chilès and Delfiner, 1999), a class of stochastic phenomena which besides second-order stationary random functions englobes also Brownian motion.

In Fig. 4, experimental and theoretical variograms of model errors are plotted. From these plots, it is possible to conclude that the stationarity assumption is fairly acceptable for the water level errors; indeed, the experimental variogram has a concave shape and it can be viewed as reaching a sill at a range below 10 km. Note nevertheless that this sill may vary in time. The second-order stationarity assumption being acceptable for the water level experimental variogram, a nested model consisting of two spherical variograms is proposed and it is possible to compute a corresponding second-order stationary covariance. In our application, the nature of the boundary conditions causes the model error to be zero in both cases. This is certainly the reason why the experimental variogram

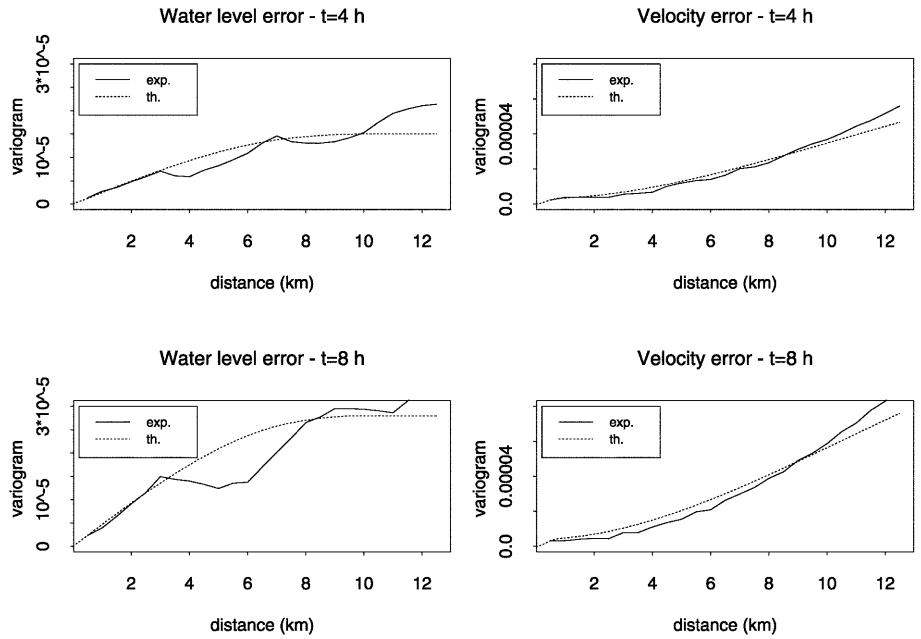

Fig. 4. Experimental (solid line) and theoretical (dashed line) variograms of model errors for water level elevation (left) and velocity (right) at different times. The water level error can be modeled with a second-order stationary variogram, while the velocity error is clearly non-stationary. The theoretical variograms are nested models

slightly increases linearly at the larger distances, phenomenon which we chose to neglect.

For the velocity error, however, the behavior of the experimental variograms shown in Fig. 4 (right) is different and the second-order stationarity assumption does not seem adequate. The variogram is not bounded (no sill apparent) and the increase of the variogram with distance is either close to quadratic or quadratic, so that it can be interpreted in two ways: either we consider a phenomenon like fractional Brownian motion which has a power variogram with an exponent lower than 2 (Yaglom, 1986) or the quadratic behavior of the variogram is explained as resulting from drift in the framework of a non-stationary model. The non-stationarity can be related to the error in the friction coefficient which generates biased model estimates. Figure 5 clearly shows such a bias, which is moreover state dependent.

A different way to tackle the problem of the interpretation of the spatial structure is to model the experimental variograms using a cubic model with a range beyond the maximal distance of computation of the experimental variogram. The phenomenon is then viewed to be second-order stationary at a larger scale than the spatial domain size. In Fig. 4 (right) the model fits the experimental variogram for the distances we are concerned with (< 25 km). Actually a nested model has been used: the first part is a cubic model with a short range which accounts for the second-order stationary part of the model error, while a second cubic model accounts for the variations at large scale. In this way we have derived an ad hoc second-order stationary covariance.

The use of a second-order stationary covariance raises difficulties, which can only be solved with strong simplifications. Especially, it is very difficult to account

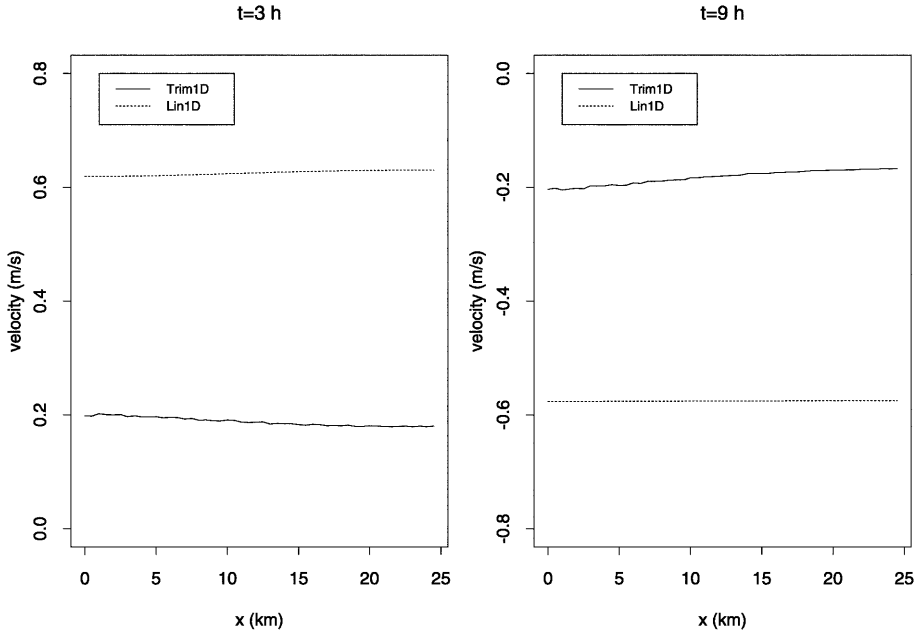

Fig. 5. Profiles of velocity computed by Trim1D (solid line) and Lin1D (dashed line) at different times. The error in the friction coefficient results in strongly biased velocity estimates. Note that this bias is state dependent

for a state dependence. An updating scheme, like the one proposed in Dee (1995), could offer a solution to this problem, but the algorithm requires that enough information is at hand, which is not the case in this example.

To summarize, we are proposing a modeling of the covariance according to the simplifying hypothesis of second-order stationarity. Since this modelization is only a coarse approximation of the real statistics, the assimilation scheme will be suboptimal (see Todling and Cohn, 1994 for a detailed discussion of suboptimal schemes). Here are the covariance functions used for the assimilation

$$Q_{\mathrm{w}}(h) = 1 \times 10^{-5}\,\mathrm{spheric}(h/7.5) + 4 \times 10^{-5}\,\mathrm{spheric}(h/10) \tag{42}$$

$$Q_{\mathrm{v}}(h) = 4 \times 10^{-6}\,\mathrm{cubic}(h/1) + 1 \times 10^{-4}\,\mathrm{cubic}(h/40) \tag{43}$$

where $\mathrm{spheric}(h) = 1 - 0.5h(3 - h^2)$ and $\mathrm{cubic}(h) = 1 - h^2[7 - h(8.75 - h^2(3.5 - 0.75h^2))]$. $|h|$ is expressed in km. Note especially that we considered for convenience the water level and the velocity errors to be independent. This is yet another simplification.

The comparison of the state estimates obtained with this modeling and the true states is shown in Fig. 6. On these time series it can be seen that although the system noise model is an approximation, the correction performed by the filter proves efficient. This is especially true for the velocity estimates: the amplitude differs now only by approximately 20% and both signals are in phase. We pointed out previously the physical meaning of an error in the phase and this is why it is important that also that part of the signal should be corrected. The correction brought for the water level estimates seems less relevant.

Although one can consider that the filter performs well in view of the approximations made in the covariance modeling, one major problem remains: the

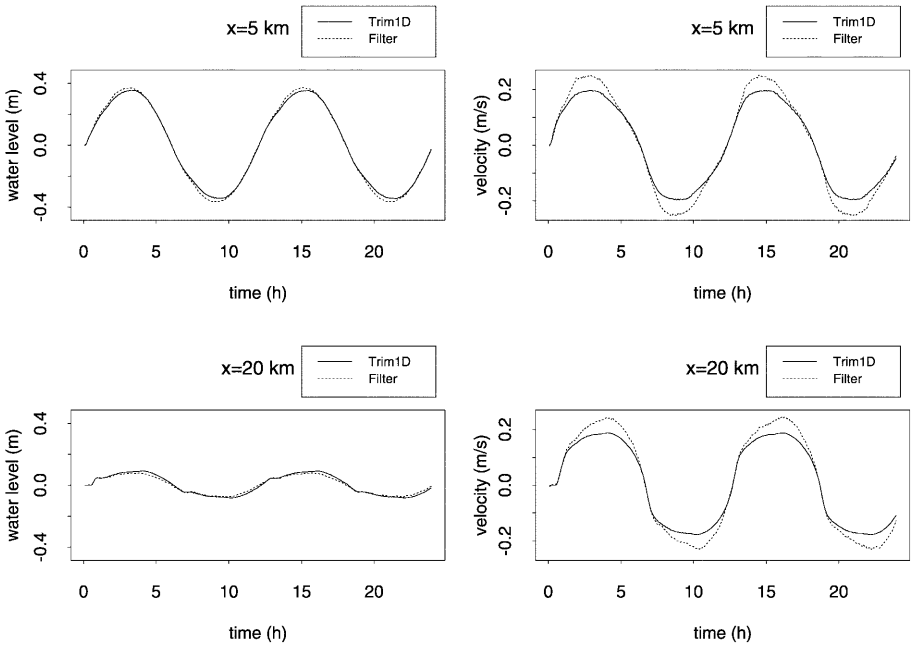

Fig. 6. Time series of water level (left) and velocity (right) for a one day run – comparison between Trim1D (solid line) and the filter (dashed line) for two different locations: $x = 5$ and 20 km. The choice of the system noise covariance model assumes second-order stationarity and steadiness of the stochastic parameters. Note that the velocity estimates are still biased, although the bias has been largely reduced

analyzed estimate is still biased. It is indeed a consequence of the Kalman filter equations (16)–(20) that if the first guess is actually biased, so remains the analyzed estimate. One can easily show that the bias of the analyzed estimate decreases, according to the following expression:

$$\overline{\mathbf{z} - \mathbf{z}^*} = (\mathbf{I}_n - \mathbf{KL})\overline{\mathbf{z} - \mathbf{z}^{\mathrm{f}}} \tag{44}$$

Figure 7 shows the true root mean square error and the filter estimated standard deviation of the estimation error, averaged over the simulation period. The influence of the estimation point is clearly visible: the estimation error at this location is a local minimum. Nevertheless, the influence area is very limited: the true root mean square error increases rapidly as soon as one gets further from the observation point. Note also the influence of the boundary conditions on the estimation error of the water level, which is minimum at the boundaries. One can clearly see on this plot that the approximate noise modeling, especially the use of steady stochastic parameters, ends in an underestimation of the velocity estimation error.

4.2
Dynamical system noise covariance modeling

In the previous paragraphs, we have proposed a covariance structure based on the hypothesis of second-order stationarity. The modeling has been performed using perfectly known model errors, which is unrealistic in practice. On the other hand, the modeling using a second-order stationary covariance turned out to be far too

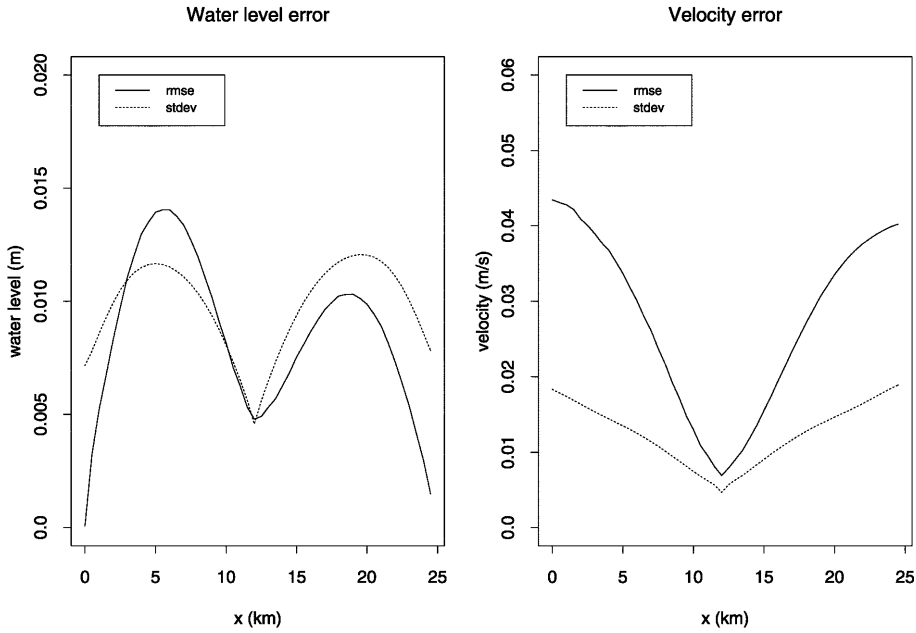

Fig. 7. True root mean square error (rmse, solid line) and filter estimated standard deviation (stdev, dashed line) of the estimation error: water level error (left) and velocity error (left). The approximate noise modeling ends in an underestimation of the velocity estimation error

approximate. These two features (feasible covariance modeling, accurate spatial structure) show the need for other tools. In Sect. 2, we stated that the system noise covariance can be divided into two independent structures: the first one accounts for an error in the physical description of the system, while the second one is a second-order stationary model. This method will now be illustrated.

What about the bias in the model? It has been previously pointed out that the error in the friction coefficient leads to a significant bias in the model. Equation (44) shows that whatever gain is used in the filter, the bias remains, though it might decrease. Therefore an explicit correction of the bias has to be undertaken. Dee and da Silva (1998) develop an algorithm to correct model bias under the assumption that there exists a subset of the observations for which the estimates are not biased. This scheme is based on the Kalman filter, where an evolution model has to be proposed for the bias and the innovations are used for the bias estimation. Then the first guess is corrected and filtered with the usual Kalman filter.

In the present application, we will consider that the model is unbiased on the mid term (that is one or two periods), so that a correction can be achieved without a specific filter. Especially, if the bias decrease of Eq. (44) enables to balance the increase due to a drift in the model error, there is no need anymore to use an additional scheme. This is however a strong assumption, which needs to be validated.

The system noise in this application is principally due to the error in the friction coefficient. Therefore it is possible to model this error, which is quite simple since the problem becomes monovariate; the matrix $\tilde{\mathbf{Q}}_k$ of Eq. (22) by the way becomes a scalar $\sigma_{\tilde{q}}^2$ (which we will consider time independent) and the matrix $\mathbf{G}_k$ reduces to a vector $\mathbf{g}_k$. The influence of the uncertainty on the state

vector is then computed via the model operator, so that the state dependence of the model error is automatically taken into account.

We use Eq. (26) in the present application, where the noise concerns the friction coefficient ($\alpha = c_f$). We take the following value for the standard deviation:

$$\sigma_{\tilde{q}_{c_f}} = 0.0006\,\mathrm{s}^{-1} \tag{45}$$

The computation of the system error covariance with such a technique seems very straightforward. Nevertheless, only a part of the system error is modeled, since only the parameter error is taken into account. In this case study, the error in the friction coefficient happens to have merely an influence on the velocity field and almost none on the water level field. This is partly due not only to the physics but also to the discretization scheme used. This feature can be easily illustrated in the extreme case of an explicit discretization, i.e. $\theta = 0$. Indeed, the discretized state equations can then be written as follows (the subscript i refers to the ith component of the variable, i.e. its value at position $i\Delta x$):

$$u_{k+1}^i = (1 - \Delta t c_f) u_k^i - g \frac{\Delta t}{\Delta x} \left(\eta_k^{i+1} - \eta_k^i\right) \tag{46}$$

$$\eta_{k+1}^i = \eta_k^i - H \frac{\Delta t}{\Delta x} \left(u_k^{i+1} - u_k^i\right) \tag{47}$$

so that the linear operator $\mathbf{G}_k$ (here a vector $\mathbf{g}_k$) becomes

$$\mathbf{g}_k s = \begin{pmatrix} -s u_k \\ 0 \end{pmatrix} \tag{48}$$

The influence on the water level in this extreme case is nil. This means in terms of Eq. (28) that $\mathbf{G}_k \tilde{\mathbf{Q}}_k \mathbf{G}_k^{\mathrm{T}}$ will not properly account for the noise related to the water level field and shows the need for an additional covariance structure. Therefore, we had proposed to add a matrix $\mathbf{Q}_k^{\mathrm{stat}}$ derived form a second-order stationary covariance function to describe the noise which cannot be directly linked to the physical description of the system. In the previous modeling experiment, we came to the conclusion that the water level error can be considered as second-order stationary and that the velocity error showed a second-order stationary part at low scale. Therefore, we use similar structures as established in Eqs. (42) and (43), i.e. the covariance functions:

$$Q_{\mathrm{w}}^{\mathrm{stat}}(h) = 1 \times 10^{-5}\,\mathrm{spheric}(h/7.5) + 4 \times 10^{-5}\,\mathrm{spheric}(h/10) \tag{49}$$

$$Q_{\mathrm{v}}^{\mathrm{stat}}(h) = 4 \times 10^{-6}\,\mathrm{cubic}(h/1) \tag{50}$$

Here again we simplify the problem by assuming that there is no cross-correlation. We could however argue that the cross-correlation is contained in the dynamical term $\mathbf{G}_k \tilde{\mathbf{Q}}_k \mathbf{G}_k^{\mathrm{T}}$.

Figure 8 shows the time series for water level and velocity estimates computed with the filter and overlaid to the true states. The dynamical modeling of the covariance turns out to take very well into account the state dependence of the model error: filtered estimates and true states now show very good agreement, the filter enabling an estimation even closer to the true state than the linear model

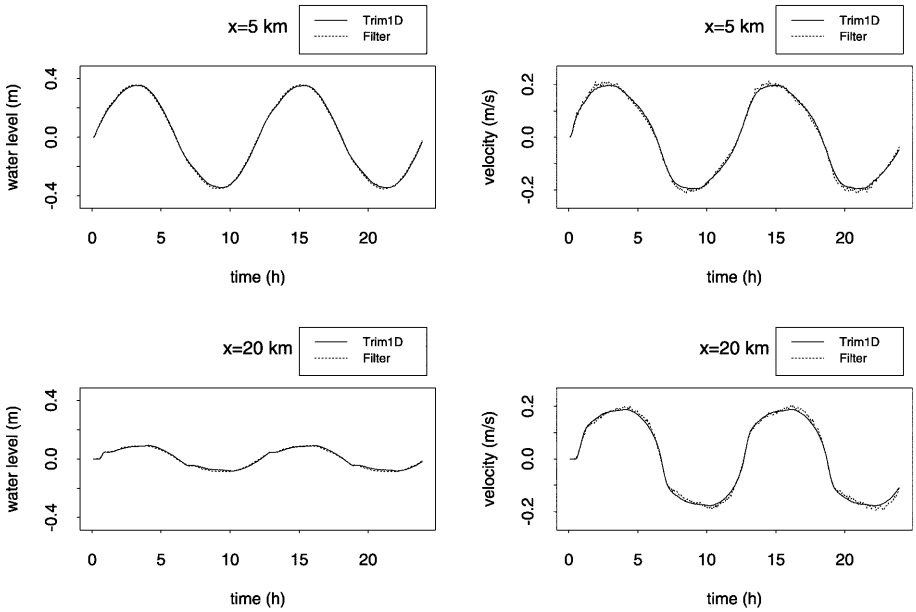

Fig. 8. Time series of water level (left) and velocity (right) for a one day run – comparison between Trim1D (solid line) and the filter (dashed line) for two different locations: $x = 5$ and 20 km. The model error covariance is now computed using the model operator, and a specific covariance model describes the second-order stationary part. The bias in the velocity estimate has been now almost fully removed

with correct friction coefficient (see Fig. 1 for comparison). Note especially that this time even the water level estimates are significantly corrected. One may nevertheless point out that the velocity field estimated with the filter is characterized by small unstabilities for the higher velocities.

The comparison between the true root mean square error and the filter estimated standard deviation of the estimation error, shown in Fig. 9, indicates how well the covariance model computed dynamically performs. Compared to the results obtained with the previous filter (see Fig. 7), the root mean square error has significantly decreased, by approximately 50% for the water level and by a factor 4 for the velocity. The influence area of the observation point is now much larger, so that the correction performed by the filter far from the observation point is significant. Moreover, the filter estimation of its own error, given by the standard deviation of the estimation error, shows a very good agreement with the true root mean square error; not only the shape of the distribution along the channel is well computed, but also the amplitude of the error.

Although the results presented here show the interest of the combined approach we proposed in Sect. 2, it would be false to conclude that the model bias problem has been fully solved. Indeed, it is still assumed in the filter equations that the model error has zero mean and therefore the filter does not correct a systematic error. We found here a way around this difficulty by considering that in the mid term the system noise has zero mean.

4.3 Discussion

We have shown in this paper the role of the model operator in generating dynamically the system noise covariance and the interest of modeling explicitly the

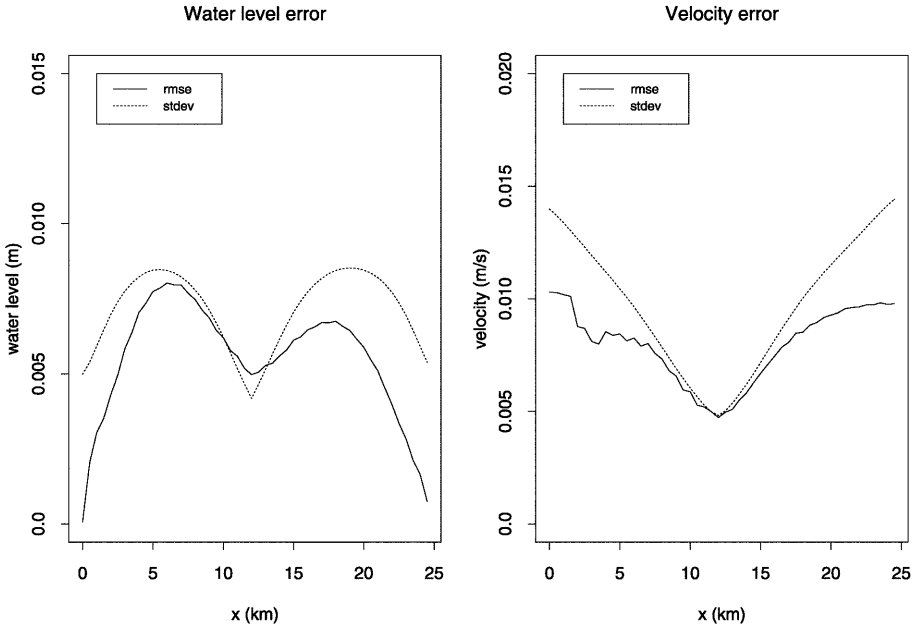

Fig. 9. True root mean square error (rmse, solid line) and filter estimated standard deviation (stdev, dashed line) of the estimation error: water level error (left) and velocity error (right). The root mean square error has significantly decreased for both variables, compared to the results obtained with the previous filter, and the filter estimates much better its own error

second-order stationary part of the noise. The advantages of this approach are twofold: on one hand, the covariance computed with the physical model enables one to describe features related to the support, such as border effects. On the other hand, the model is automatically updated, so that the state dependence of the model error is automatically integrated in the covariance model. This last point turned out very powerful to reduce efficiently the model bias introduced by error in the friction coefficient.

Lastly, we would like to illustrate the basically different behavior of the two filters described in this work. For this purpose, the Kalman gains computed by each one are compared. The Kalman gain, whose expression is given by Eq. (18), is an $n \times m$ matrix, where n is the dimension of the state vector and m the number of the measurements assimilated. In our application, $n = 100$ and $m = 2$. It is then possible to measure the contribution of the measurement z_j^{o} to the correction of the first guess z_i^{f}; this is exactly K_{ij}.

In Fig. 10, the coefficients corresponding to the contribution of the two measurements to the correction of the first guess at position $x = 5$ km are plotted. In the case where the noise covariance is modeled with a steady second-order stationary covariance, the gain converges to a steady state, which is a well known property of the Kalman filter when the numerical model is linear and the different parameters are steady. Conversely, when a dynamically updated system noise covariance is introduced, the gain is state dependent. This means that the correction performed by the filter is better adapted to the actual first guess error. Since in our case the evolution of the system is periodic, so is the gain. Note especially that the extremal values of the coefficients correspond approximately to the situations of extremal model error (see Fig. 2 for comparison).

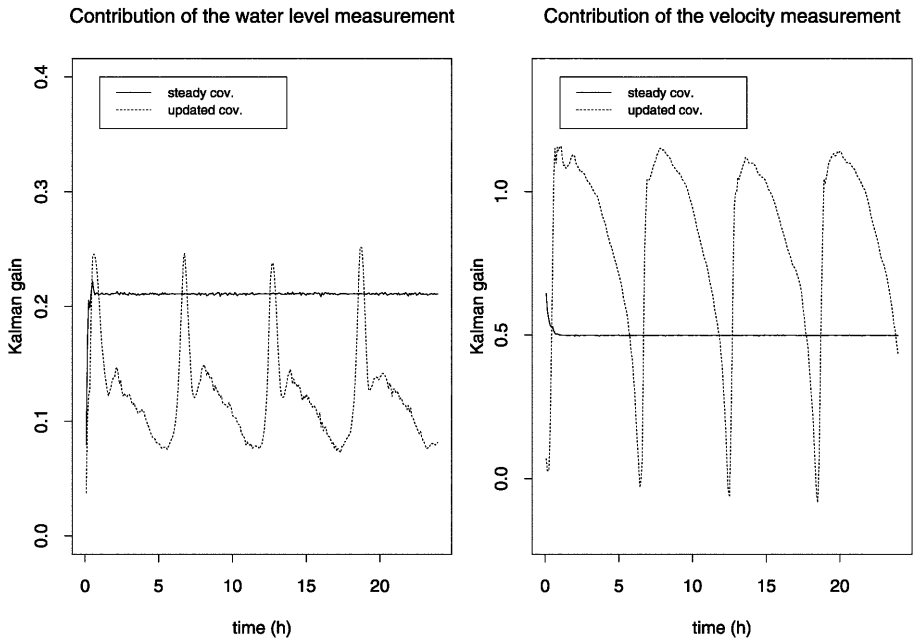

Fig. 10. Contribution of the water level measurement to the correction of the estimation of water level at position $x = 5$ km and of the velocity measurement to the correction of the estimation of velocity at position $x = 5$ km. Using a steady covariance model for the system noise causes the Kalman gain to converge to a steady state (solid line), while the gain computed with a dynamically updated covariance (dashed line) is state dependent and better adapted to the actual estimation error

5
Summary and conclusion

In systems where only little information is available to determine the spatial covariance of the variable, the second-order stationarity assumption is a practical necessity which enables to assess a covariance model and eventually to estimate its parameters. Nevertheless, we showed that even in simple cases the structure of the model error is more complex. Our discussion relied on a twin experiment where a full shallow water model simulated the true state and a Kalman filter has been used to correct a linear model with an erroneous friction coefficient. This experiment enabled us to have access to the real model error, and the spatial variograms of the water level and velocity errors showed a non second-order stationary behavior. The existence of a drift was moreover an indication that the velocity estimates were biased in the short term.

To cope with this practical difficulty, we proposed to make use of the dynamical model to account for the largest part of the error. In this approach, the model error is divided into two terms: the first one is the contribution of the uncertainties which can be directly linked to a physical parameter, whereas the second represents low-scale errors, which have been considered second-order stationary. This method, referred to as *dynamical system noise modeling*, presents the advantage that the system error covariance relies in a natural way upon the system state.

The method, applied to one-dimensional hydrodynamics, proved to be very efficient: the water level and velocity estimates showed very good agreement with

the reference state, and the bias has been largely reduced. Moreover, the description of the estimation error provided by the analyzed covariance matrix turned out to be very accurate. This is an important issue in real applications, where there is a need to validate the simulations. Finally, one particular feature of this modeling is a better adaptation to the system state: whereas the Kalman gain computed with steady statistics converge to a steady state, the Kalman gain obtained with dynamical modeling showed higher values in cases where the estimation error was maximal.

In the case study, we implemented the Kalman filter with a linear hydrodynamical model, since we wanted to compare the results in cases where the Kalman filter is supposed to work well. Further, we would like to mention that the modeling described here has proven efficient too when used with a reduced rank square root filter proposed by Verlaan and Heemink (1995) and a non-linear three-dimensional shallow water model. Results from that work will be reported later.

Finally, this paper aims to be a first step to a more geostatistical approach of data assimilation. The parallelism between Kalman filtering and cokriging has been clearly emphasized: the assimilation step is equivalent to a cokriging of the innovations. This motivates to consider the advantages offered by the theory of regionalized variables as well as variographical analysis, which relies merely on the study of the spatial structure of the measurements.

References

Bennett AF (1992) Inverse Methods in Physical Oceanography. Cambridge University Press, Cambridge, UK

Cañizares R (1999) On the application of data assimilation in regional coastal models. PhD Thesis, Delft University of Technology, 133 p

Casulli V (1995) Numerical methods for free surface hydrodynamics. Technical Report, Laboratorio di Mathematica Applicata, Dipartemento di Ingegneria Civile ad Ambientale, Trento, Italy, 56 p

Casulli V, Cattani E (1992) Stability, accuracy and efficiency of a semi-implicit method for three-dimensional shallow water flow. Comput. Math. Appl., 27(4): 99–112

Chauvet P (1999) Aide-mémoire de géostatistique linéaire. Presses de l'Ecole des Mines de Paris, Paris, France

Chilès JP, Delfiner P (1999) Geostatistics: Modeling Spatial Uncertainty. Wiley, New York, USA

d'Andréa Novel B, Cohen de Lara M (1994) Commande Linéaire des Systèmes Dynamiques. Masson, Paris, France

Daley R (1991) Atmospheric Data Analysis. Cambridge University Press, Cambridge, UK

Dee DP (1992) A simple scheme for tuning forecast error covariance matrices. In proceedings of the variational assimilation, with special emphasis on three-dimensional aspects, 191–205, European Centre for Medium-Range Weather Forecasts Reading, UK (available from http://dao.gsfc.nasa.gov/DAO_people/dee)

Dee DP (1995) On-line estimation of error covariance parameters for atmospheric data assimilation. Mon. Wea. Rev., 123(4): 1128–1145

Dee DP, da Silva AM (1998) Data assimilation in the presence of forecast bias. Quart. J. R. Met. Soc., 124: 269–295

Dee DP, da Silva AM (1999) Maximum-likelihood estimation of forecast and observation error covariance parameters, part 1: methodology. Mon. Wea. Rev., 124: 1822–1834

Dee DP, Gaspari G, Redder G, Rukhovets L, da Silva AM (1999) Maximum-likelihood estimation of forecast and observation error covariance parameters, part 2: applications. Mon. Wea. Rev., 124: 1835–1849

Eigbe U, Beck MB, Wheather HS, Hirano F (1998) Kalman filtering in ground water flow modelling: problems and prospects. Stochastic Hydrol. Hydraul., 12: 15–32

Eknes M, Evensen G (1999) An ensemble Kalman filter with a 1-d marine ecosystem model, submitted to JMS

Evensen G (1992) Using the extended Kalman filter with a multilayer quasi-geostrophic ocean model. J. Geophys. Res., 97: 17905–17924
Evensen G (1995) Sequential data assimilation with a nonlinear quasi-geostrophic model using Monte Carlo methods to forecast the error statistics. J. Geophys. Res., 99-C5: 10143–10162
Evensen G, Dee DP, Schröter J (1998) Parameter estimation in dynamical models. In Chassignet EP, Verron J (eds) Ocean Modeling and Parameterizations, 373–398, Kluwer Academic Publishers, Amsterdam, Netherlands
Evensen G, van Leeuwen PJ (2000) An ensemble kalman smoother for nonlinear dynamics. Mon. Wea. Rev., 128: 1852–1867
Gaspari G, Cohn SE (1999) Construction of correlation functions in two and three dimensions. Quart. J. R. Meteol. Soc., 125: 723–757

Journel AG, Huijbregts CJ (1978) Mining Geostatistics. Academic Press, London, UK
Maybeck PS (1979) Stochastic Models, Estimation and Control. Academic Press, New York
Pedlosky J (1987) Geophysical Fluid Dynamics. Springer-Verlag, New York, USA
Rosenthal W, Wolf T, Witte G, Buchholz W, Rybaczok P (1998) Measured and modelled water transport in the Odra estuary for the flood period July/August 1997. Germ. J. Hydr., 50(2/3): 215–230
Sénégas J (1999) Hydrodynamical modeling and data assimilation within the Odra estuary. External report GKSS/99/E/42, GKSS, Geesthacht, Germany
Todling R, Cohn SE (1994) Suboptimal schemes for atmospheric data assimilation based on the Kalman filter. Mon. Wea. Rev., 122: 2530–2557
Verlaan M (1998) Efficient Kalman filtering algorithms for hydrodynamic models. PhD Thesis, Delft University of Technology, Netherlands
Verlaan M, Heemink AW (1995) Reduced rank square root filters for large scale data assimilation problems. In Second International Symposium on Assimilation of Observations in Meteorology and Oceanography, World Meteorological Organization, Geneva, Switzerland, pp. 247–252
Verlaan M, Heemink AW (1999) Non-linearity in data assimilation applications: a practical method for analysis. Mon. Wea. Rev., submitted (available from http://ta.twi.tudelft.nl/users/verlaan)
Wackernagel H (1998) Multivariate Geostatistics. Springer-Verlag Berlin, Germany
Yaglom AM (1986) Correlation Theory of Stationary and Related Random Functions. Springer-Verlag, Berlin, Germany